



## Article

# Characterization of Novel Multifunctional Xylanase from Rumen Metagenome and Its Effects on In Vitro Microbial Fermentation of Wheat Straw

Moguang Zhang <sup>†</sup>, Qinghua Qiu <sup>†</sup> , Xianghui Zhao <sup>\*</sup>, Kehui Ouyang and Chanjuan Liu <sup>\*</sup>

Jiangxi Province Key Laboratory of Animal Nutrition, Engineering Research Center of Feed Development, Jiangxi Agricultural University, Nanchang 330045, China; zmg18702590979@sina.com (M.Z.); rcauqqh@cau.edu.cn (Q.Q.); ouyangkehui@sina.com (K.O.)

<sup>\*</sup> Correspondence: xianghuizhao@jxau.edu.cn (X.Z.); chanjuanhx@jxau.edu.cn (C.L.)

<sup>†</sup> These authors contributed equally to this work.

**Abstract:** This study investigated the characterization of a novel multifunctional enzyme, RuXyn394, derived from the metagenome of beef cattle rumen, and its impact on the in vitro microbial fermentation of wheat straw. RuXyn394, a member of the glycosyl hydrolase 11 family, displayed optimal activity under diverse pH and temperature conditions: xylanase at pH 5.5 and 50 °C, acetyl esterase at pH 6.5 and 60 °C, exoglucanase at pH 7.0 and 50 °C, and endoglucanase at pH 6.0 and 50 °C. The enzyme's xylanase, endoglucanase, and exoglucanase activities exhibited remarkable pH stability across the range of pH 3–8 and maintained a relatively stable performance at temperatures from 20 to 50 °C, 20 to 60 °C, and 20 to 70 °C, respectively. The xylanase function, with the highest  $k_{cat}/K_m$  ratio, was identified as the predominant activity of RuXyn394. The enzyme's various functions responded uniquely to metal ions; notably, the addition of 5 mM  $K^+$  significantly boosted the activities of xylanase, exoglucanase, and endoglucanase by 55.5%, 53.5%, and 16.4%, respectively, without affecting its acetyl esterase activity. Over the course of three time points (30 min, 60 min, 120 min), the degradation products of wheat straw xylan, including xylopentaose, xylohexaose, xyloheptaose, xylobiose, xylose, and total xylooligosaccharides, constituted an average of 18.4%, 33.7%, 20.6%, 22.9%, 4.3%, and 95.7% of the total products, respectively. RuXyn394 effectively hydrolyzed wheat straw, resulting in augmented volatile fatty acid production and ammonia-N levels during in vitro microbial fermentation. These findings indicate the potential of RuXyn394 as a novel and highly efficient enzyme preparation, offering promising prospects for the valorization of wheat straw, an agricultural by-product, in ruminant diets.

**Keywords:** multifunctional enzyme; rumen metagenome; wheat straw; microbial fermentation



**Citation:** Zhang, M.; Qiu, Q.; Zhao, X.; Ouyang, K.; Liu, C. Characterization of Novel Multifunctional Xylanase from Rumen Metagenome and Its Effects on In Vitro Microbial Fermentation of Wheat Straw.

*Fermentation* **2024**, *10*, 574.

<https://doi.org/10.3390/fermentation10110574>

Academic Editor: Penka Petrova

Received: 24 September 2024

Revised: 6 November 2024

Accepted: 7 November 2024

Published: 10 November 2024



**Copyright:** © 2024 by the authors. Licensee MDPI, Basel, Switzerland. This article is an open access article distributed under the terms and conditions of the Creative Commons Attribution (CC BY) license (<https://creativecommons.org/licenses/by/4.0/>).

## 1. Introduction

As the global population and economy grow, the demand for meat and dairy is steadily increasing, driving up the need for forage [1]. In some regions, a shortage of this type of feed restricts livestock farming development. Wheat straw, the leftover stems after wheat harvest, is often seen as waste [2]. Burning and direct field incorporation are common methods for managing these waste materials [2,3]. However, burning imposes significant environmental pressure, contributing to air pollution, greenhouse gas emissions, and ecosystem disruption [3]. On the other hand, field incorporation may easily trigger outbreaks of pests and diseases, while the excessive decomposition of straw results in the overproduction of organic acids, damaging the root systems of crops [4,5]. Wheat straw contains valuable fibrous materials like cellulose and hemicellulose, making it potential forage for ruminants. Using wheat straw as forage not only optimizes resources and safeguards the environment but also cuts breeding costs for ruminants, supporting sustainable agriculture. However, the efficiency of utilizing wheat straw by ruminants is hindered by



conserved domain. For homologous modeling of RuXyn394, the Phyre2 server employed 3WP6 as a template.

### 2.3. Expression of RuXyn394

The proficient *E. coli* BL21 (DE3) cells underwent a transformation process using the recombinant pET-RuXyn394 plasmid. Afterward, the resulting transformed cells were cultivated on LB agar plates with added kanamycin at 37 °C. Once confirmed by PCR, the transformants were introduced into 2 mL of LB liquid medium. Following an overnight culture, a 250 µL aliquot was transferred into 25 mL of LB medium for shaking cultivation at 37 °C until reaching an optical density at 600 nm of approximately 0.8. The expression of RuXyn394 was induced by isopropyl-β-D-thiogalactoside (IPTG) at a final concentration of 0.3 mM, maintained at 20 °C, 80 rpm, for 20 h. Meanwhile, non-transformed *E. coli* BL21 (DE3) cells served as a concurrent control. The cultures were centrifuged at 8000 rpm for 15 min, and the resulting pellets were resuspended in phosphate-buffered saline (PBS) after discarding the supernatant. Ultrasonic treatment in an ice-water bath followed, producing a RuXyn394-containing supernatant analyzed via SDS-PAGE stained with Coomassie Blue. For purification, Ni-charged affinity chromatography was utilized. Following ultrasonic disruption and centrifugal separation, the resulting supernatant was mixed with pH 8.0 binding buffer (comprising 0.05 M sodium dihydrogen phosphate and 0.3 M sodium chloride) to achieve dilution, which was then applied to a 5 mL Bio-Scale Mini Nuvia IMAC Ni-Charged column (Bio-Rad, Hercules, CA, USA) within a low-pressure chromatography setup (Biologic LP from Bio-Rad, Hercules, CA, USA) at a flow rate of 1.0 mL/min. Subsequently, the bound RuXyn394 was initially washed with binding buffer containing 0.02 M imidazole and later eluted using binding buffer containing 0.25 M imidazole. The eluted liquid with RuXyn394 was quantified using a Bradford Protein Assay Kit (Sangon Biotech, Shanghai, China). SDS-PAGE confirmed the purity of RuXyn394. It is worth noting that despite multiple purification steps in this experiment, it was not possible to completely remove all contaminating proteins. However, these contaminants do not affect the subsequent enzymatic characterization analysis.

### 2.4. Characterization of RuXyn394

The substrate specificity of RuXyn394 was elucidated through analyses of reaction mixtures containing 1% wheat straw xylan [14], 0.0725% p-nitrophenylacetate (*p*-NPA) (N814797, Macklin, Shanghai, China), 1% chitosan (A600614, Sangon Biotech, Shanghai, China, deacetylation ≥ 90%), 1% sodium carboxymethylcellulose (CMC-Na) (30036328, Sinopharm Chemical Reagent Co., Ltd., Shanghai, China), or 1% Avicel (11365, Sigma-Aldrich, Shanghai, China), incubated at 50 °C and pH 6.0 (0.05 M citric acid-disodium hydrogen phosphate buffer) for durations of 30 min, 10 min, 2 h, 2 h, or 2 h, respectively. The quantification of liberated reducing sugars was facilitated by a reagent comprising alkaline 3,5-dinitrosalicylic acid, with colorimetric intensity assessed at 540 nm [15]. The liberated p-nitrophenol was quantified using a colorimetric method at 410 nm.

The influence of pH on the activity of purified RuXyn394 was ascertained within a 0.05 M citric acid-disodium hydrogen phosphate buffer system spanning pH 3.0 to 8.0 at 50 °C, utilizing wheat straw xylan, *p*-NPA, chitosan, CMC-Na, or Avicel as substrates, as previously described. The optimal temperature for the RuXyn394's activity was assessed by employing wheat straw xylan, *p*-NPA, chitosan, CMC-Na, or Avicel as substrates, within their respective optimal pH, varying between 20 and 80 °C. The activity related to pH and temperature variations was presented as relative activity, capped at a maximum of 100%. RuXyn394's resistance to heat and pH was assessed by subjecting it to pre-incubation at temperatures ranging from 20 to 80 °C for 1 h, and at pH ranging from 3.0 to 8.0 for 2 h at 4 °C, respectively, after which its remaining activity was measured at optimal pH and temperature.

The specific activities of RuXyn394's xylanase, acetyl esterase, exoglucanase, and endoglucanase functions were determined under optimal conditions: xylanase activity

was evaluated using 1% wheat straw xylan at 50 °C and pH 5.5 for 30 min; acetyl esterase activity with 0.0725% *p*-NPA at 60 °C and pH 6.5 for 10 min; exoglucanase activity with 1% Avicel at 50 °C and pH 7.0 for 2 h; and endoglucanase activity with 1% CMC-Na at 50 °C and pH 6.0 for 2 h. The enzymatic activity, defined as one unit (U), corresponded to the amount of enzyme capable of producing 1 μmol of reducing sugars or *p*-nitrophenol per min. Specific activity was expressed as units per milligram protein. To determine the  $K_m$  and  $V_{max}$  values of RuXyn394, nonlinear regression analysis employing the Michaelis–Menten equation was conducted. The substrates used varied from 0.2% to 2.5% wheat straw xylan, 0.5 mM to 8 mM *p*-NPA, 0.1 to 8.0% Avicel, and 0.125 to 2.0% CMC-Na. GraphPad Prism v5.0 (GraphPad Software Inc., San Diego, CA, USA) was utilized for this analytical process.

To investigate the resistance of RuXyn394's four enzymatic functions to metal ions, inhibitors, and detergents, a specific quantity of these substances was individually introduced into the reaction system. Subsequently, the reaction was conducted as previously described. The enzymatic activity in the absence of any substance additions served as the baseline, denoted as 100%.

### 2.5. Hydrolysis Products of Wheat Straw Xylan

A reaction system with a volume of 1 mL was utilized in this study, consisting of 1% wheat straw xylan and 1.12 μg RuXyn394 (approximately 0.2 U of xylanase activity). The reaction was conducted for 30 min, 60 min, and 120 min, respectively, at 50 °C and pH 5.5. A control group was also established, which contained inactivated RuXyn394. The resulting hydrolysis products (xylose, xylobiose, xylotriose, xyloetraose, and xylopentaose) were analyzed using an HPLC system (model D-7000, Hitachi Ltd., Tokyo, Japan), following our previous methodology [15].

### 2.6. Hydrolysis of Wheat Straw by RuXyn394

This study explored the effects of varying RuXyn394 dosages on wheat straw hydrolysis. Wheat straw at 5% concentration was incubated with RuXyn394 enzyme levels from 0.15 to 2.25 μg in a 2 mL system at 50 °C and pH 5.5 for 12 h. Released reducing sugars were analyzed, with a control using an inactive enzyme.

### 2.7. In Vitro Fermentation

A study was conducted to assess RuXyn394's impact on the microbial fermentation of wheat straw through in vitro methods. The methodology involved utilizing microbial inocula from bovine feces, as outlined in our prior publications [13]. In summary, healthy beef cattle were fed a diet comprising 700 g/kg wheat straw and 300 g/kg concentrates, and fresh feces were collected. The feces (450 g) were then diluted in 1 L of buffered McDougal's artificial saliva, stirred at 39 °C for approximately 25 min, and filtered through two layers of cheesecloth. Subsequently, fermentation took place in 120 mL serum bottles, each containing 500 mg wheat straw and 60 mL fecal inoculum. For enzyme treatment, 187 μg of purified RuXyn394 was added to the fermentation bottle, while an equal amount of inactivated RuXyn394 served as the control. The bottles were incubated in triplicate in a shaking bath at 39 °C for 48 h. To halt the fermentation process, the bottles were placed on ice. The resulting fermentation mixture underwent filtration with nylon bags, and the filtrate was then subjected to analysis for pH, volatile fatty acids (VFA), and ammonia-N, following previous research [16].

### 2.8. Statistical Analyses

The statistical analysis employed IBM SPSS statistics version 20 (IBM, Chicago, IL, USA). For comparisons involving three or more groups, a one-way analysis of variance (ANOVA) was applied. Multiple comparisons were conducted using the least significant difference (LSD) test, and for comparisons between two groups, an independent-sample *t*-test was utilized. Statistical significance was established at  $p < 0.05$ .

### 3. Results

#### 3.1. Sequence Analysis of RuXyn394

The RuXyn394 gene consists of 1182 base pairs and codes for a protein of 393 amino acids, as revealed by sequencing analysis. The anticipated theoretical molecular mass for this protein is 42 kDa. BLAST [protein] analysis of EMBL-EBI (<https://www.ebi.ac.uk/services>) using the UniProtKB/Swiss-Prot Database with default parameters revealed that RuXyn394 had a higher identity with some xylanase sequences from *Neocallimastix patriciarum* (UniProtKB accession Q9UV68) (60.3%), *Piromyces* sp. (UniProtKB accession Q12667) (64.9%), *N. patriciarum* (UniProtKB accession B8YG19) (63.2%), and *Fibrobacter succinogenes* (UniProtKB accession P35811) (46.7%) in the GH11 family at the amino acid level. A phylogenetic tree of RuXyn was generated by analyzing 20 protein sequences through BLAST. The results revealed a significant genetic affinity between RuXyn394 and the endo-1,4-beta-xylanases identified in *F. succinogenes* (UniProtKB accession P35811), as illustrated in Figure 1A. The GH11 domain was pinpointed via InterPro analysis within amino acid residues 60 to 266, as depicted in Supplementary Figure S1. The conserved patterns and specific elements within the RuXyn394 sequence were determined through aligning it with multiple similar protein sequences sharing distinctive characteristics. Based on the aligned proteins, the catalytic sites are represented by two residues, E155 and E253, both indicated with a pentacle. Employing the homology modeling technique, the 3D structure of RuXyn394 was constructed utilizing Phyre2, with 3WP6 as the reference template (Figure 1B). The anticipated configuration of RuXyn394 exhibited a  $\beta$ -jelly-roll fold reminiscent of a partially closed hand, a characteristic trait observed in enzymes belonging to the GH11 family.

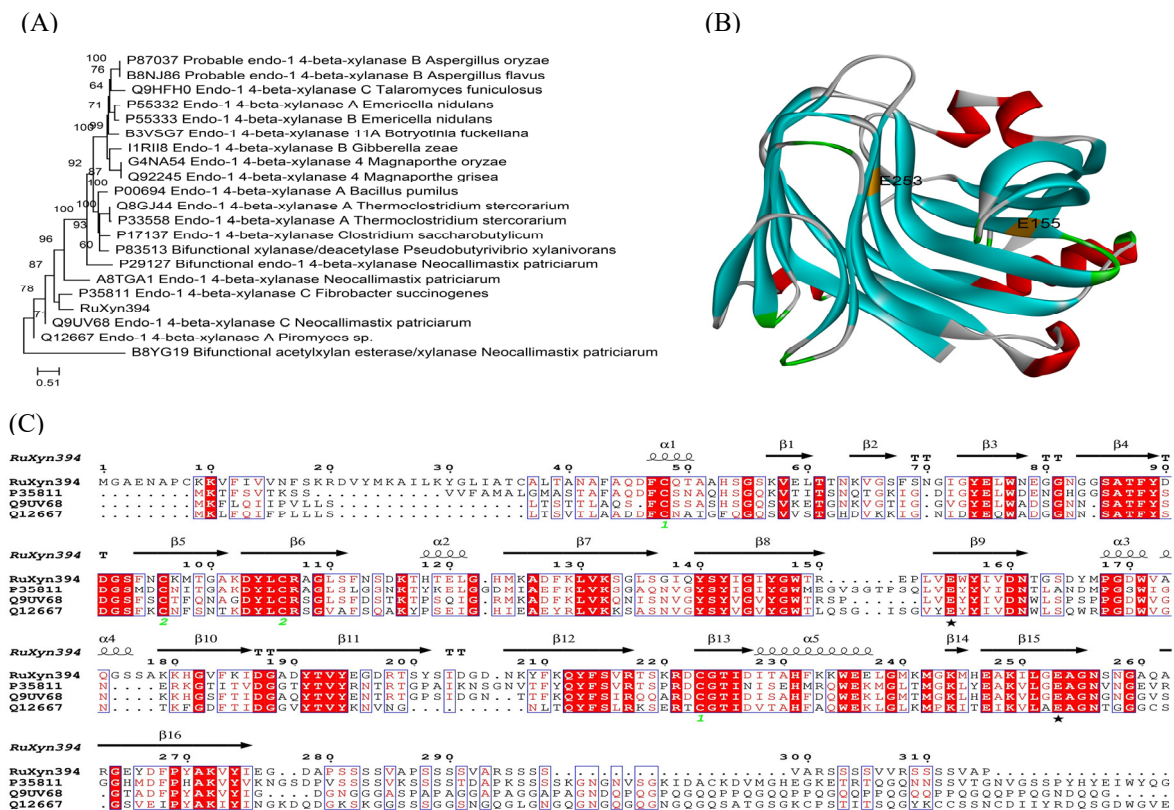


**Figure 1.** The phylogenetic tree (A), homology modeling (B), and multialignment analysis (C) of RuXyn394. (A) The phylogenetic tree was constructed using the neighbor-joining method. The

RuXyn394 was aligned online (<https://www.ebi.ac.uk/services>) using the UniProtKB/Swiss-Prot database. The first 20 similar sequences obtained were selected to construct the phylogenetic tree by MEGA X software. (B) The homology modeling of RuXyn394 was performed using GH11 xylanase from *N. patriciarum* (PDB number 3WP6) as the template. Red indicated alpha helices, light blue indicated beta-sheets, gray indicated disordered coils, and E253 and E155 were putative catalytic residues. (C) Multiple alignments of RuXyn394 and several GH11 xylanases from *N. patriciarum* (UniProtKB accession Q9UV68), *Piromyces* sp. (UniProtKB accession Q12667), and *Fibrobacter succinogenes* (UniProtKB accession P35811) were performed using ClustalW. Putative catalytic residues (pentacle).

### 3.2. Expression and Characteristics of RuXyn394

The gene encoding RuXyn394 was expressed in a heterologous host, *E. coli* BL21 (DE3). SDS-PAGE analysis of the purified protein revealed a distinct band corresponding to approximately 44 kDa, aligning with the calculated theoretical molecular mass of RuXyn394 based on its amino acid sequence (Figure 2).

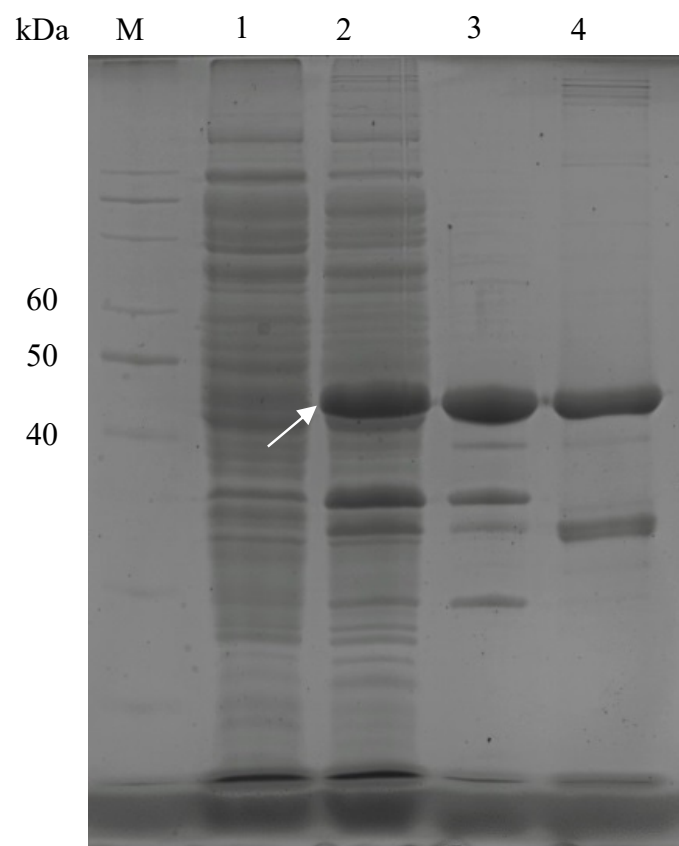


**Figure 2.** Analysis of RuXyn394 by SDS-PAGE. M, protein marker; 1, non-transformed *E. coli* BL21 (DE3); 2, RuXyn394 transformants induced with 0.3 mM IPTG; 3 and 4, purified RuXyn394 from different collection tubes. Arrow indicates expressed RuXyn394.

RuXyn394's substrate specificity was assessed with xylan, Avicel, CMC-Na, chitosan, and *p*-NPA. The enzyme showed a marked preference for xylan degradation, with notable activity against *p*-NPA, Avicel, and CMC-Na, while its activity on chitosan was negligible (Figure 3). Subsequently, this study investigated the characteristics of RuXyn394 using xylan, Avicel, CMC-Na, and *p*-NPA as substrates.

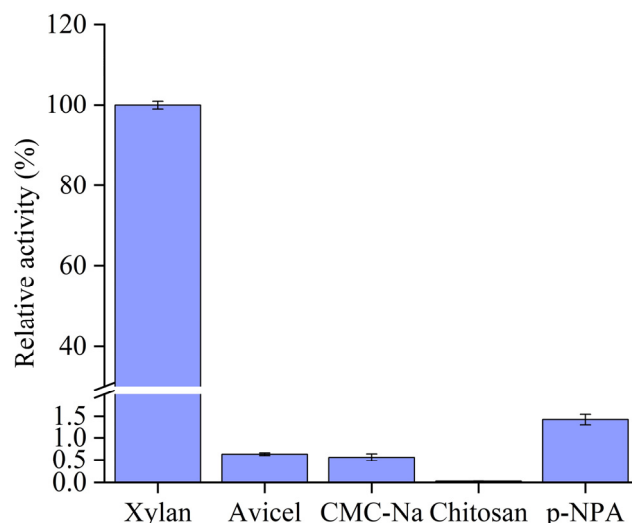


**Figure 3.** The substrate specificity of RuXyn394. The activity of RuXyn394 towards various substrates was expressed as relative activity, with the activity towards xylan set as 100%. In this experiment, when xylan was used as the substrate, the activity of RuXyn394 was 65.3 U/mg.

The activity of RuXyn394 with xylan, *p*-NPA, Avicel, and CMC-Na as substrates exhibits a distinct pH-dependent profile (Figure 4A). For xylan, RuXyn394's optimal activity is at pH 5.5, with over 80% retained from pH 5.0 to 6.5. However, the activity falls below 25% beyond pH 8.0 or below 4.5, with near-complete inactivation below pH 4.0. With *p*-NPA, peak activity occurs at pH 6.5, with over 60% maintained from pH 5.5 to 6.5, and sharply declines beyond pH 5.0 or 7.0, nearly inactivating below pH 4.5. With Avicel, RuXyn394 exhibits its highest activity at pH 7.0, retaining over 75% activity from pH 6.0 to 8.0, but drops below 10% below pH 5.5. Unlike the aforementioned three substrates, when CMC-Na served as the substrate, RuXyn394's activity peaked at pH 6.0 and retained over 50% activity from pH 5.0 to 8.0, with over 80% maintained between pH 4.0 and 7.0. After a 2 h pre-treatment within pH 3.0–8.0, RuXyn394 retained over 70% of its maximum activity using xylan, Avicel, and CMC-Na substrates (Figure 4B). Yet, with *p*-NPA as the substrate, it maintains 70% or more activity only under pH 5.0–7.0 after the same pre-treatment duration.

The temperature dependence of RuXyn394 at the optimal pH using four substrates is shown in Figure 4C. Utilizing xylan, Avicel, and CMC-Na as substrates, RuXyn394 demonstrated peak activity at 50 °C. For xylan, more than 60% of this activity is retained across temperatures from 20 °C to 70 °C. Similarly, CMC-Na maintains over 60% activity from 20 °C to 80 °C, while Avicel preserves over 50% activity within the 40 °C to 70 °C range. With *p*-NPA, RuXyn394 exhibited maximum activity at 60 °C; however, except at 50 °C, RuXyn394 maintained activity below 60% at other temperatures utilized in this study. For thermal stability, RuXyn394 was subjected to pre-treatment at 20–80 °C for 1 h. The findings reveal that when utilizing xylan as a substrate, RuXyn394 maintains over 80% activity after a 1 h pre-treatment at 20–50 °C, but undergoes complete deactivation beyond 60 °C (Figure 4D). In the case of the *p*-NPA substrate, pre-treated RuXyn394 demonstrates activity ranging from 41% to 78%, with temperature-induced variations showing some perplexing patterns. When CMC-Na is the substrate, RuXyn394's residual activity after a 1 h pre-treatment at 20–40 °C remains relatively stable. However, after pre-treatment at 50 and 60 °C, the residual activity increases by 155% and 36%, respectively. Nevertheless, as the pre-treatment temperature rises to 70 and 80 °C, RuXyn394's residual activity decreases by 23% and 48%, respectively. Similarly, with Avicel as the substrate, RuXyn394's residual activity surged by 143% following a 1 h pre-treatment at 50 °C. This activity notably declined with pre-treatment temperatures exceeding 70 °C, approaching inactivation at 80 °C.

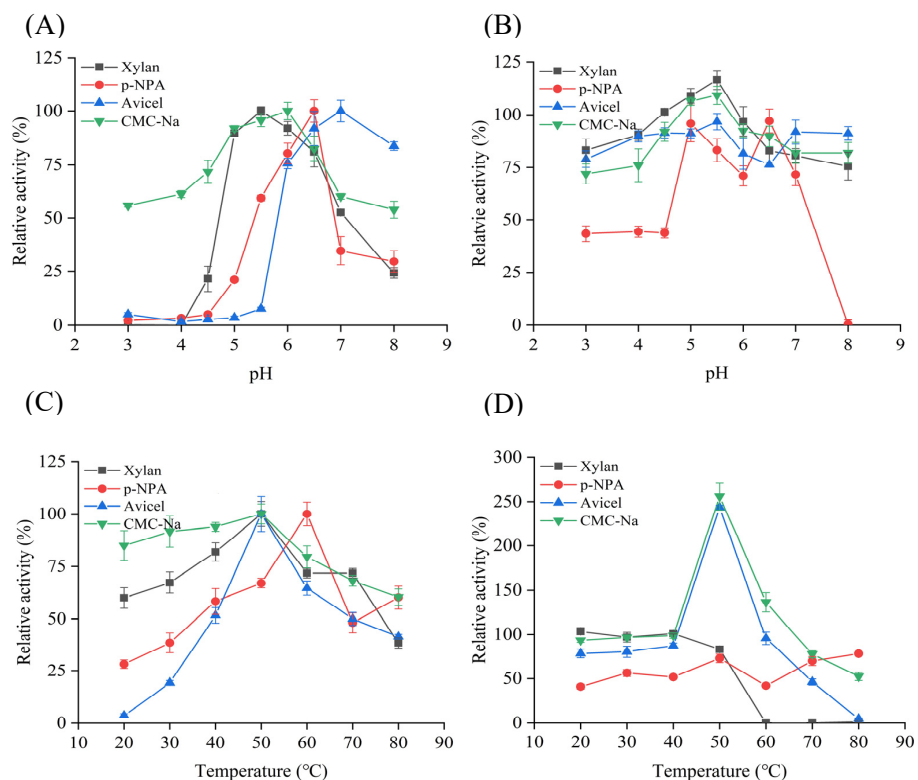


**Figure 4.** Analysis of RuXyn394’s pH dependency (A) and stability (B), as well as its temperature dependency (C) and stability (D). Substrate concentration was 1% (*w/v*) wheat straw xylan, 0.0725% *p*-NPA, 1% CMC-Na, or 1% Avicel. (A) Reactions were carried out in 0.05 M citric acid-disodium hydrogen phosphate buffer system spanning pH 3.0 to 8.0 at 50 °C. (B) Reactions were carried out in their respective optimal pH, varying between 20 and 80 °C. Activity related to pH and temperature variations was presented as relative activity, capped at maximum of 100%. RuXyn394’s resistance to heat (C) and pH (D) was assessed by subjecting it to pre-incubation at 20–80 °C for 1 h, and at pH 3.0–8.0 for 2 h at 4 °C, respectively, after which its remaining activity was measured at optimal pH and temperature.

The effects of various metal ions, inhibitors, and detergents on RuXyn394 activity are summarized in Figure 5. When xylan was employed as the detection substrate,  $Mg^{2+}$ ,  $Ca^{2+}$ ,  $Ni^{2+}$ ,  $Zn^{2+}$ , and  $Mn^{2+}$  exhibited notable inhibitory effects on RuXyn394 activity at both 1 mM and 5 mM concentrations. Conversely,  $Cu^{2+}$  at 1 mM,  $K^+$  at 5 mM, and  $Na^+$  at 5 mM enhance RuXyn394 activity by 25%, 55%, and 65%, respectively. SDS and Triton-X100 exhibit a modest inhibitory effect (<50%) on RuXyn, whereas EDTA demonstrates pronounced inhibition, nearly abolishing RuXyn activity even at a concentration as low as 1 mM. The addition of 1 mM and 5 mM DTT resulted in an approximately 11% increase in the RuXyn activity. When utilizing *p*-NPA as a substrate, the activity of RuXyn increased by 21%, 28%, 11%, and 42% respectively in the presence of 1 mM  $Ca^{2+}$ , 5 mM  $Na^+$ , 1 mM EDTA, and 1 mM Tween20. Other additives exhibited either no significant effect or varying degrees of inhibitory effects on RuXyn activity at two concentrations. When utilizing Avicel as a substrate, at 1 mM,  $Mg^{2+}$ ,  $Na^+$ ,  $Ni^{2+}$ ,  $Mn^{2+}$ , and SDS enhanced the activity of RuXyn394 by 28%, 128%, 23%, 157%, and 156%, respectively, yet this enhancement markedly diminished, with  $Mg^{2+}$  even exhibiting strong inhibition as concentrations rose to 5 mM. Additionally, 1 mM  $K^+$  inhibited RuXyn394 activity by 70%, while 5 mM  $K^+$  increased its activity by 53%. DTT, EDTA, Tween-20, and Triton X100 all demonstrated significant inhibitory effects on RuXyn394 regardless of the concentration tested. When utilizing CMC-Na as a substrate, 1 mM and 5 mM  $K^+$  and  $Zn^{2+}$  increased RuXyn activity by 10–16%, while 1 mM  $Ni^{2+}$  significantly boosted activity by 70%. Other ions, inhibitors, and detergents showed either negligible impact or different levels of inhibition on RuXyn.

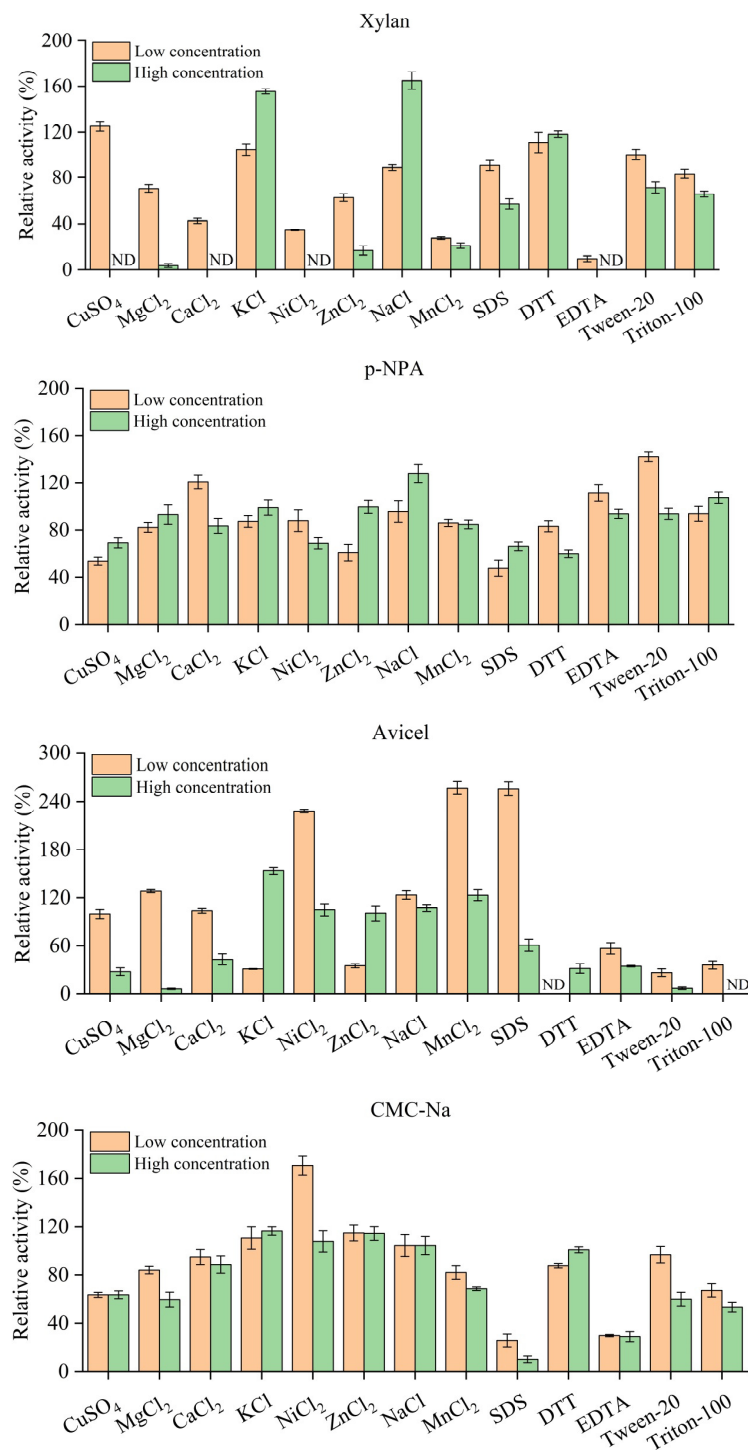


**Figure 5.** The effects of metal ions, inhibitors, and detergents on RuXyn394 activity across different substrates. The activity without additives was taken as 100%. For metal ions, SDS, DTT, and EDTA, the terms “low concentration” and “high concentration” refer to final concentrations of 1 mM and 5 mM, respectively, in the reaction system. For Tween-20 and Triton-100, “low concentration” and “high concentration” refer to final concentrations of 0.1% and 0.5% (v/v), respectively, in the reaction system. The activity without additives was taken as 100%.

RuXyn394 exhibited the highest  $k_{cat}/K_m$  ratio for wheat straw xylan among the four substrates (Table 1), indicating the strongest catalytic efficiency for this particular substrate. This finding aligns with the observed peak activity of RuXyn when wheat straw xylan served as the substrate.

**Table 1.** Kinetic parameters of RuXyn394.

Substrates	$K_m$ (mg mL <sup>-1</sup> )	$V_{max}$ (μmol min <sup>-1</sup> mg <sup>-1</sup> )	$k_{cat}/K_m$ (mL mg <sup>-1</sup> S <sup>-1</sup> )	Specific Activity (U/mg)
Wheat straw xylan	5.30	262.2	34.7	190.2
<i>p</i> -NPA	0.077	3.2	29.2	3.03
Avicel	85.27	11.6	0.10	0.79
CMC-Na	11.82	0.76	0.05	0.30

### 3.3. Hydrolysis Products of Wheat Straw Xylan

The hydrolysis products of wheat straw xylan by RuXyn394 were analyzed in the present study. Regardless of the reaction time, xylo-tetraose and xylose were the highest and lowest sugar products obtained, respectively (Figure 6; Supplementary Figure S2). Increasing the reaction time from 30 to 120 min significantly increased xylopentaose, xylo-tetraose, and total XOS by 179.6, 311.5, and 675.9 μg/mL, respectively. The XOS distribution was also investigated. Except for xylo-triose, the proportions of other individual sugars and the total XOS was not significantly influenced by the reaction time. However, the proportion of xylo-triose notably decreased from 23.6% to 19.2% and 19.1% as the reaction time increased from 30 min to 60 min and 120 min, respectively. Across the three time points, xylopentaose, xylo-tetraose, xylo-triose, xylobiose, xylose, and the total XOS accounted for an average of 18.4%, 33.7%, 20.6%, 22.9%, 4.3%, and 95.7%, respectively.

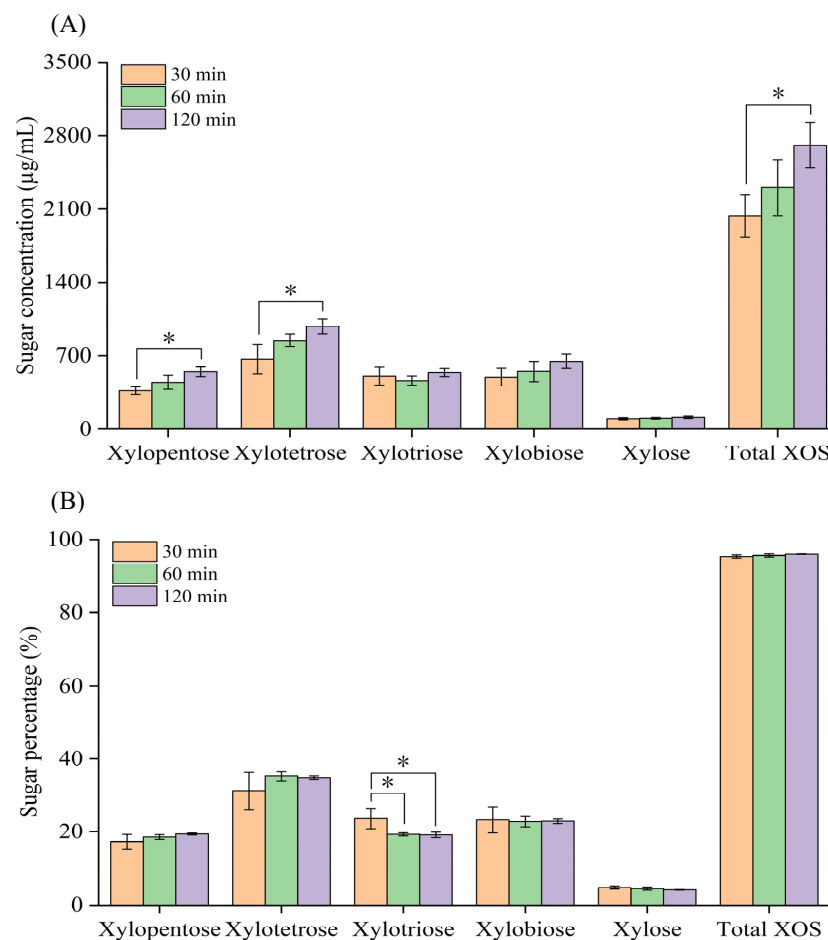


**Figure 6.** Effects of RuXyn394 on production (A) and percentage (B) of XOS with incubation times of 30, 60, and 120 min. Within same metrics, asterisk indicates significant differences ( $p \leq 0.05$ ).

### 3.4. Hydrolysis and In Vitro Ruminal Fermentation of Wheat Straw

Figure 7A depicted the hydrolysis of wheat straw treated with a varying dosage of RuXyn394. With the increment of RuXyn from 0.15 to 2.25  $\mu\text{g}$  in the reaction system, the reducing sugar yield from wheat straw hydrolysis significantly rose from 37.8 to 181.3  $\mu\text{g}/\text{mL}$ . In order to assess the capacity of RuXyn394 to enhance the efficiency of straw digestion in ruminants, we examined the influence of RuXyn supplementation on the in vitro microbial fermentation process using wheat straw as the substrate. The addition of RuXyn394 resulted in several significant changes compared to the control group (Figure 7B). The pH in the RuXyn394 group is approximately 0.11 units lower than in the control group (6.49 vs. 6.38,  $p = 0.001$ ). In terms of VFA production, RuXyn394 led to an increase of approximately 11.06 mM in total VFA concentration. Acetate levels rose by about 8.12 mM, propionate by approximately 2.64 mM, and butyrate by around 0.31 mM in the RuXyn394 group. Furthermore, the RuXyn394 group exhibited an increase of approximately 1.35 mM in  $\text{NH}_3\text{-N}$  concentration.

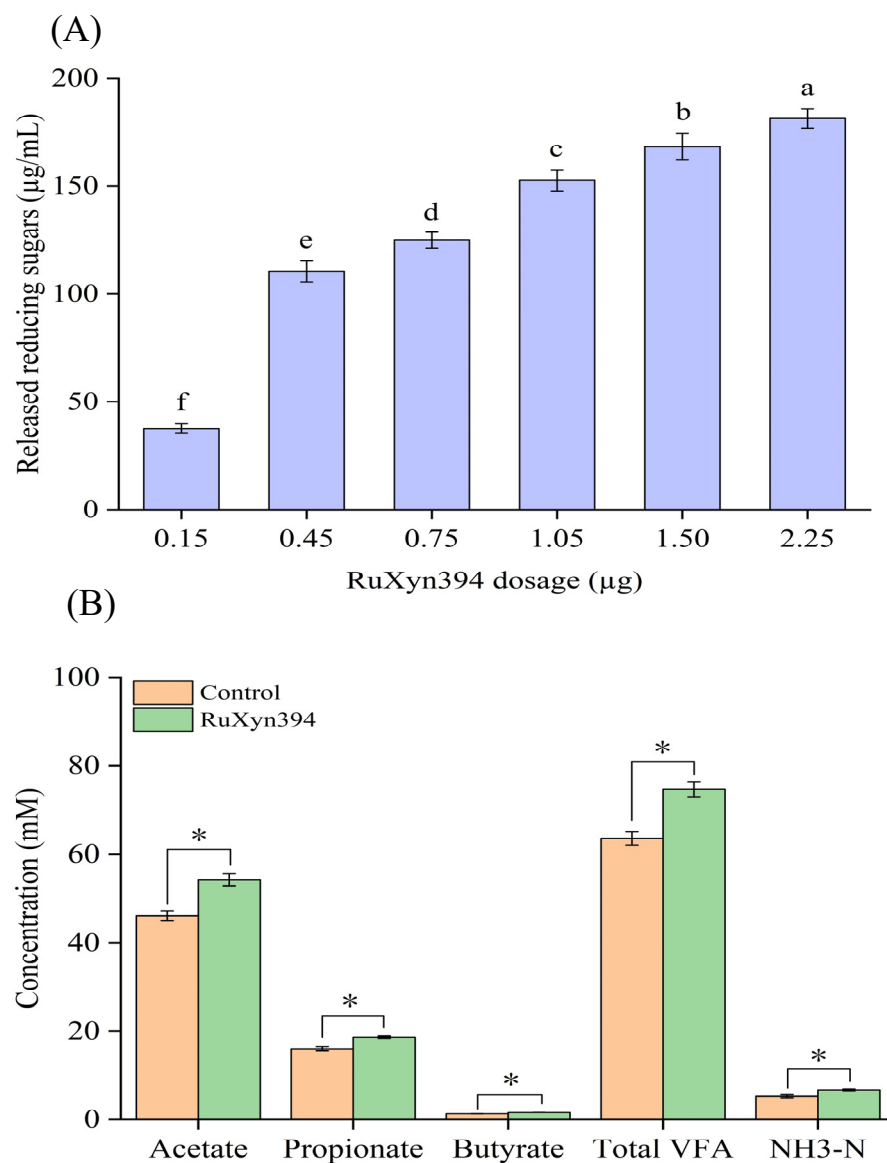


**Figure 7.** Effects of RuXyn394 on hydrolysis (A) and in vitro microbial fermentation (B) of wheat straw. Significant differences ( $p \leq 0.05$ ) are indicated by different lowercase letters and asterisks.

#### 4. Discussion

Agricultural straws serve as primary forage for ruminants. However, the intricate lignin–hemicellulose–cellulose composite structure in the cell wall poses a challenge for degradation and utilization by rumen microorganisms. Notably, xylan is the primary component of straw hemicellulose. Degrading xylan not only enhances hemicellulose utilization but also promotes the effective degradation and utilization of cellulose. Building on this, our study discovered the multifunctional xylanase RuXyn394 in the rumen, examining its enzymatic properties and its impact on the microbial fermentation of wheat straw.

The phylogenetic analysis indicated a proximate association between RuXyn394 and a GH 11 family xylanase from *F. succinogenes*. *F. succinogenes*, a prominent cellulolytic species in the rumen, has the ability to produce a diverse array of cellulolytic enzymes, such as hemicellulase, cellulase, and carbohydrate esterase, and plays a crucial role in the ruminal degradation of fiber [17]. The outcomes align with the observation that RuXyn394 originates from the rumen of beef cattle. InterPro analysis and homology modeling both confirmed that RuXyn394 belongs to the GH 11 family.

RuXyn394’s significant activity towards wheat straw xylan, p-NPA, Avicel, and CMC-Na indicates its functionality as a xylanase, acetyl esterase, endoglucanase, and exoglucanase. These enzymatic functionalities demonstrate markedly different properties. RuXyn394’s four enzymatic functions peaked between pH 5.5 and 7.0, which is somewhat consistent with the pH range of 6.0 to 7.0 typically found in the rumen environment [18,19]. The optimal temperatures for the xylanase, endoglucanase, and exoglucanase activities of RuXyn394 are all 50 °C. Despite the optimal temperature exceeding that of the rumen, similar findings have been reported for a multifunctional xylanase/glucanase characterized by Loaces et al. (2016) from the bovine rumen [20] (Table 2) or for other rumen-derived xylanase [15,21]. In the current study, the xylanase, endoglucanase, and exoglucanase functions of RuXyn394 demonstrated excellent pH stability, aligning with reports of certain multifunctional enzymes from previous studies [22] (Table 2). In terms of thermostability, the xylanase, exoglucanase, and endoglucanase functions of RuXyn394 maintained relatively ideal stability at temperatures ranging from 20 to 50 °C, 20 to 60 °C, and 20 to 70 °C, respectively. Notably, after a 2 h pre-treatment at 50 °C, the activities of the exoglucanase and endoglucanase of RuXyn394 increased by 143% and 155%, respectively. Despite our attempts to find a plausible explanation for this outcome, regrettably, none was identified. However, similar phenomena have been observed in previous studies [23,24], although the authors of those studies did not analyze or discuss them.

**Table 2.** Summary of some multifunctional cellulolytic enzymes from rumen microorganisms.

Protein Name	Resource	Characteristics and Kinetic Parameters		Function	Reference
		Substrate	Optimal pH, Temperature		
EndoG	Rumen metagenome	p-NPC	5.0, 50 °C	Xylanase, glucanase	[20]
KG51	Goat rumen metagenome	CMC	5.0, 50 °C	endo-β-1,4-glucanase, endo-β-1,4-mannosidase, endo-β-1,4-Xylanase	[25]
		Beechwood xylan	5.0, 40 °C		
		Avicel	N/A		
N/A	Buffalo rumen metagenome	Locust bean gum Xylan Pectin CMC	5.0 and 6.0, 35 °C N/A N/A N/A	Xylanase, pectin esterase, endoglucanase, mannanase	[26]
XynS20E	Ruminal fungus Neocallimastix patriciarum	Birchwood (xylanase)	5.8, 49 °C	Xylanase, acetylxylan esterase	[27]
		Birchwood xylan (acetylxylan esterase)	8.2, 58 °C		

Table 2. Cont.

Protein Name	Resource	Characteristics and Kinetic Parameters		Function	Reference
		Substrate	Optimal pH, Temperature		
CbGH5	Cattle dung	CMC	9.0, 90 °C	Xylanase, cellulase	[28]
		Birchwood xylan	8.0, 90 °C		
RfGH5_4	Ruminococcus flavefaciens FD-1 v3	CMC-Na	5.5, 55 °C	Glucanase, xylanase	[29]
		β-D-glucan	N/A		
		Tamarind Xyloglucan	N/A		
		Avicel	N/A		
		Birchwood xylan	N/A		
CelXyn2	Buffalo rumen metagenome	CMC	6.0, 45 °C	Endoglucanase, xylanase	[30]
		beechwood xylan	6.0, 45 °C		
XylR	Nelore cattle rumen	Beechwood xylan	6.5, 37 °C	endo-1,4-β-xylanase, esterase	[31]
		p-nitrofenyl acetate	N/A		
RuCelA	Yak rumen metagenome	CMC	5.0, 50 °C	Xylanase, endoglucanase	[22]
		Birchwood xylan	7.0, 65 °C		
RuXyn394	Beef cattle rumen metagenome	Wheat straw xylan	5.5, 50 °C	Xylanase, acetyl esterase, exoglucanase, endoglucanase	This study
		p-NPA	6.5, 60 °C		
		Avicel	7.0, 50 °C		
		CMC-Na	6.0, 50 °C		

SA: specific activity; N/A: not available.

RuXyn394’s various functions exhibited distinct responses to the metal ions, inhibitors, and detergent selected in the present study. Overall, however, the acetyl esterase activity was relatively less affected by these additives compared to the other three functions. Specific concentrations of Cu<sup>2+</sup>, K<sup>+</sup>, and Na<sup>+</sup> demonstrated a significant enhancement of RuXyn394’s xylanase activity, aligning with partial characteristics of some xylanases from rumen microorganisms [32]. The exoglucanase activity of RuXyn394 is notably boosted by low concentrations of Ni<sup>2+</sup>, Mn<sup>2+</sup>, SDS, and K<sup>+</sup>. This finding suggests that these metal ions may be pivotal in catalytic activity, possibly through interactions with key amino acid residues in the enzyme’s active site, serving as cofactors, or by causing conformational changes in the enzyme’s three-dimensional structure [33,34]. These results were in line with some of the partial characteristics of bifunctional cellobiohydrolase/xylanase and cellobiohydrolase/β-xylosidase from *Chaetomium thermophilum* and the mangrove soil metagenome, respectively [35,36]. However, unlike RuXyn394, SDS nearly completely inactivates these two enzymes. SDS, an anionic surfactant, is a potent agent that denatures proteins and is known to affect the sensitivity of the majority of enzymes [15,37]. In the current study, both the xylanase and exoglucanase activities of RuXyn394 exhibit considerable resistance to low concentrations of SDS. The inactivation of xylanase by SDS solutions has been reported before [37,38]. SDS resistance is a shared feature among proteins that maintain a stable structure, as they possess few conformations that are vulnerable to protease activity and exhibit inherent resistance against enzymatic breakdown [39]. Apart from SDS and EDTA, the endoglucanase activity of RuXyn394 exhibits good resistance to other additives used in this study, and it is notably enhanced by low concentrations of Ni<sup>2+</sup>. EDTA also demonstrates a significant inhibitory effect on the xylanase and exoglucanase activities of RuXyn394, suggesting that these enzymatic functions may require metal ions as cofactors [40]. This is corroborated by the promotional effects of many metal ions on the

activity of RuXyn394, as previously mentioned. Taking into account the four functions of RuXyn394, it may be possible to enhance its activity by incorporating an appropriate level of  $K^+$  or  $Na^+$  into the reaction system.

RuXyn394's highest  $k_{cat}/K_m$  value, with wheat straw xylan, indicates its superior catalytic efficiency for this substrate, confirming xylanase as its principal activity. This correlates with the enzyme's peak performance on wheat straw xylan. Among its activities, RuXyn394's xylanase outperforms its exo- and endoglucanase activities, consistent with other reported rumen-derived multifunctional xylanases [22,41].

Given the strong xylanase activity of RuXyn394, we conducted a detailed analysis of the degradation products resulting from its action on xylan. The results revealed that among the five analyzed products, the yield of xylose was minimal, with the average XOS production accounting for 95.7%. XOS, known for their health benefits and prebiotic effects, particularly enhance beneficial gut bacteria and exhibit a range of activities including antioxidant, antimicrobial, anti-inflammatory, and antiallergic properties, as well as aiding in metabolic improvements for diabetes [15]. Their applications span functional foods and additives for both human and animal production. Therefore, RuXyn394 holds significant potential for XOS production in the food and feed industries.

Our initial goal in isolating RuXyn394 was to enhance the utilization of crop straw by degrading xylan within the cellulose–hemicellulose–lignin complex. The findings indicate that RuXyn394's multifunctionality, particularly its activity in degrading microcrystalline cellulose, makes it an attractive candidate for the hydrolysis of agricultural straws. This is because, compared to the amorphous regions, the dense crystalline areas of cellulose in lignocellulosic substrates are also a key factor that limit the efficient degradation of cellulose by rumen microorganisms and their enzymes [42,43]. Exoglucanase is very important for the degradation of crystalline cellulose due to its unique ability to target and degrade the highly ordered crystalline regions [44]. Numerous investigations have revealed that the combined action of exoglucanase with cellulase and xylanase significantly amplifies the enzymatic breakdown of agricultural straws [45,46]. In addition, the deacetylation of xylan by acetyl esterase can enhance xylanase accessibility and hydrolysis in pre-treated wheat straw, while the solubilization of xylan improves cellulose exposure to cellulases, amplifying its hydrolysis [47]. The aforementioned studies show that xylanase, endoglucanase, exoglucanase, and acetyl esterase each play a vital, constructive, and synergistic role in the degradation of straw lignocelluloses. This confers a substantial advantage to RuXyn394 in straw degradation, as evidenced by the significant increase in the reduction of sugars produced from wheat straw hydrolysis with the escalated dosage of RuXyn394 in the current research.

Rumen volatile fatty acids (VFAs), key end-products, primarily arise from the microbial fermentation of dietary carbohydrates such as cellulose, hemicellulose, pectin, starch, and soluble sugars [48]. The observed increase in VFAs could be attributed to the expedited enzymatic breakdown of wheat straw nutrients by RuXyn394, facilitating the easier microbial degradation of components like cellulose and hemicellulose. Studies have shown that the addition of exogenous xylanases can enhance the *in vitro* ruminal fermentation of wheat straw, boosting VFA yield and fiber digestibility [11,12], which aligns with our findings. Moreover, RuXyn394 has been shown to notably elevate the concentration of  $NH_3-N$ , a reflection of the equilibrium between dietary protein breakdown and nitrogen assimilation by rumen microbes [12], potentially due to enhanced nitrogen degradation by RuXyn394. In summary, RuXyn394 has been effective in enhancing the microbial fermentation process of wheat straw.

## 5. Conclusions

From rumen metagenomics, we identified and expressed a multifunctional enzyme, RuXyn394, characterized as a xylanase/acetylsterase/exoglucanase/endoglucanase, with a focus on xylanase activity in *E. coli*. RuXyn394's activities peaked at various pH and temperature combinations: xylanase at pH 5.5 and 50 °C, acetylsterase at pH 6.5 and 60 °C,

exoglucanase at pH 7.0 and 50 °C, and endoglucanase at pH 6.0 and 50 °C. The enzyme's xylanase, endoglucanase, and exoglucanase activities displayed remarkable pH stability, while its exoglucanase and endoglucanase functions showed relatively good thermostability. The addition of K<sup>+</sup> and Na<sup>+</sup> further boosted RuXyn394's activity. The primary hydrolysis products from wheat straw xylan by RuXyn394 were XOS, including xylobiose, xylotriose, xylotetraose, and xylopentaose, constituting an average of 95.7% of the total products analyzed. RuXyn394 effectively broke down wheat straw, and its supplementation led to increased VFA production and NH<sub>3</sub>-N levels during in vitro microbial fermentation, potentially enhancing the straw's nutritional value for ruminants and rendering it a more suitable feed. Overall, as an exogenous enzyme, RuXyn394 holds significant promise for enhancing microbial fermentation and the utilization of wheat straw in ruminants.

**Supplementary Materials:** The following supporting information can be downloaded at: <https://www.mdpi.com/article/10.3390/fermentation10110574/s1>, Figure S1: InterPro analysis of RuXyn394; Figure S2: HPLC profile for the RuXyn394 group, control group, and standard substance.

**Author Contributions:** M.Z.: methodology, resources, formal analysis, investigation, writing—original draft. C.L. and Q.Q.: resources. K.O. and X.Z.: project administration, funding acquisition. C.L.: conceptualization, writing—original draft, writing—review and editing, funding acquisition. All authors have read and agreed to the published version of the manuscript.

**Funding:** The current study was funded by the Natural Science Foundation of Jiangxi Province (20224ACB205007, 20242BAB20309), the Project of Jiangxi Provincial Department of Education (GJJ2200414), the Key Research and Development Projects of Jiangxi Province (20232BBF60009, 20232BBF60010), and the National Natural Science Foundation of China (31760687).

**Data Availability Statement:** The original contributions presented in the study are included in the article, further inquiries can be directed to the corresponding authors.

**Conflicts of Interest:** The authors declare no conflicts of interest.

## References

1. Oenema, O.; de Klein, C.; Alfaro, M. Intensification of grassland and forage use: Driving forces and constraints. *Crop Pasture Sci.* **2014**, *65*, 524–537. [[CrossRef](#)]
2. Devi, S.; Gupta, C.; Jat, S.L.; Parmar, M. Crop residue recycling for economic and environmental sustainability: The case of India. *Open Agric.* **2017**, *2*, 486–494. [[CrossRef](#)]
3. Porichha, G.K.; Hu, Y.; Rao, K.T.V.; Xu, C.C. Crop residue management in India: Stubble burning vs. other utilizations including bioenergy. *Energies* **2021**, *14*, 4281. [[CrossRef](#)]
4. Yu, F.; Chen, Y.; Huang, X.; Shi, J.; Xu, J.; He, Y. Does straw returning affect the root rot disease of crops in soil? A systematic review and meta-analysis. *J. Environ. Manag.* **2023**, *336*, 117673. [[CrossRef](#)]
5. Liu, X.; Dou, S.; Zheng, S. Effects of Corn Straw and Biochar Returning to Fields Every Other Year on the Structure of Soil Humic Acid. *Sustainability* **2022**, *14*, 15946. [[CrossRef](#)]
6. Rémond, C.; Aubry, N.; Crônier, D.; Noël, S.; Martel, F.; Roge, B.; Rakotoarivonina, H.; Debeire, P.; Chabbert, B. Combination of ammonia and xylanase pretreatments: Impact on enzymatic xylan and cellulose recovery from wheat straw. *Bioresour. Technol.* **2010**, *101*, 6712–6717. [[CrossRef](#)]
7. Isci, A.; Thieme, N.; Lamp, A.; Zverlov, V.; Kaltschmitt, M. Production of xylo-oligosaccharides from wheat straw using microwave assisted deep eutectic solvent pretreatment. *Ind. Crops Prod.* **2021**, *164*, 113393. [[CrossRef](#)]
8. Chen, H.; Zhao, X.; Liu, D. Relative significance of the negative impacts of hemicelluloses on enzymatic cellulose hydrolysis is dependent on lignin content: Evidence from substrate structural features and protein adsorption. *ACS Sustain. Chem. Eng.* **2016**, *4*, 6668–6679. [[CrossRef](#)]
9. Dos Santos, J.P.; da Rosa Zavareze, E.; Dias, A.R.G.; Vanier, N.L. Immobilization of xylanase and xylanase-β-cyclodextrin complex in polyvinyl alcohol via electrospinning improves enzyme activity at a wide pH and temperature range. *Int. J. Biol. Macromol.* **2018**, *118*, 1676–1684. [[CrossRef](#)]
10. Hu, J.; Arantes, V.; Saddler, J.N. The enhancement of enzymatic hydrolysis of lignocellulosic substrates by the addition of accessory enzymes such as xylanase: Is it an additive or synergistic effect? *Biotechnol. Biofuels* **2011**, *4*, 36. [[CrossRef](#)]
11. Togtokhbayar, N.; Cerrillo, M.A.; Rodríguez, G.B.; Elghandour, M.M.; Salem, A.Z.; Urankhaich, C.; Jigidpurev, S.; Odongo, N.E.; Kholif, A.E. Effect of exogenous xylanase on rumen in vitro gas production and degradability of wheat straw. *Anim. Sci. J.* **2015**, *86*, 765–771. [[CrossRef](#)] [[PubMed](#)]

12. Li, L.; Qu, M.; Liu, C.; Xu, L.; Pan, K.; Song, X.; Ouyang, K.; Li, Y.; Zhao, X. Expression of a recombinant *Lentinula edodes* xylanase by *Pichia pastoris* and its effects on ruminal fermentation and microbial community in in vitro incubation of agricultural straws. *Front. Microbiol.* **2018**, *9*, 2944. [[CrossRef](#)] [[PubMed](#)]
13. Hristov, A.N.; McAllister, T.A.; Cheng, K.J. Effect of dietary or abomasal supplementation of exogenous polysaccharide-degrading enzymes on rumen fermentation and nutrient digestibility. *J. Anim. Sci.* **1998**, *76*, 3146–3156. [[CrossRef](#)]
14. Hu, D.; Zhao, X. Characterization of a new xylanase found in the rumen metagenome and its effects on the hydrolysis of wheat. *J. Agric. Food Chem.* **2022**, *70*, 6493–6502. [[CrossRef](#)]
15. Li, T.; Lei, X.; Wang, L.; Liu, C.; Qiu, Q.; Li, Y.; Song, X.; Xiong, X.; Zang, Y.; Qu, M.; et al. Production of xylo-oligosaccharides with degree of polymerization 3–5 from wheat straw xylan by a xylanase derived from rumen metagenome and utilization by probiotics. *Food BioSci.* **2023**, *56*, 103360. [[CrossRef](#)]
16. Zhang, X.; Lei, X.; Ouyang, K.; Zhang, W.; Liu, C.; Li, Y.; Qiu, Q.; Zang, Y.; Qu, M.; Pan, K. Characteristics of a recombinant *Lentinula edodes* ferulic acid esterase and its adverse effects on in vitro fermentation of wheat straw. *Fermentation* **2023**, *9*, 683. [[CrossRef](#)]
17. Jun, H.; Qi, M.; Ha, J.; Forsberg, C. *Fibrobacter succinogenes*, a dominant fibrolytic ruminal bacterium: Transition to the post genomic era. *Asian-Australas. J. Anim. Sci.* **2007**, *20*, 802–810. [[CrossRef](#)]
18. Castro-Costa, A.; Salama, A.; Moll, X.; Aguiló, J.; Caja, G. Using wireless rumen sensors for evaluating the effects of diet and ambient temperature in nonlactating dairy goats. *J. Dairy Sci.* **2015**, *98*, 4646–4658. [[CrossRef](#)]
19. Kaur, R.; Garcia, S.; Horadagoda, A.; Fulkerson, W. Evaluation of rumen probe for continuous monitoring of rumen pH, temperature and pressure. *Anim. Prod. Sci.* **2010**, *50*, 98–104. [[CrossRef](#)]
20. Loaces, I.; Bottini, G.; Moyna, G.; Fabiano, E.; Martínez, A.; Noya, F. EndoG: A novel multifunctional halotolerant glucanase and xylanase isolated from cow rumen. *J. Mol. Catal. B Enzym.* **2016**, *126*, 1–9. [[CrossRef](#)]
21. Wang, Q.; Luo, Y.; He, B.; Jiang, L.S.; Liu, J.X.; Wang, J.K. Characterization of a novel xylanase gene from rumen content of Hu sheep. *Appl. Biochem. Biotechnol.* **2015**, *177*, 1424–1436. [[CrossRef](#)] [[PubMed](#)]
22. Chang, L.; Ding, M.; Bao, L.; Chen, Y.; Zhou, J.; Lu, H. Characterization of a bifunctional xylanase/endoglucanase from yak rumen microorganisms. *Appl. Microbiol. Biotechnol.* **2011**, *90*, 1933–1942. [[CrossRef](#)] [[PubMed](#)]
23. da Silva, P.O.; de Alencar Guimarães, N.C.; de Carvalho Peixoto-Nogueira, S.; Betini, J.H.; Marchetti, C.R.; Zanoelo, F.F.; de Moraes, M.d.L.T.; Marques, M.R.; Giannesi, G.C. Production of cellulase-free xylanase by *Aspergillus flavus*: Effect of polyols on the thermostability and its application on cellulose pulp biobleaching. *Afr. J. Biotechnol.* **2015**, *14*, 3368–3373. [[CrossRef](#)]
24. Sá-Pereira, P.; Mesquita, A.; Duarte, J.C.; Barros, M.R.A.; Costa-Ferreira, M. Rapid production of thermostable cellulase-free xylanase by a strain of *Bacillus subtilis* and its properties. *Enzym. Microb. Technol.* **2002**, *30*, 924–933. [[CrossRef](#)]
25. Lee, K.-T.; Tousehik, S.H.; Baek, J.-Y.; Kim, J.-E.; Lee, J.-S.; Kim, K.-S. Metagenomic mining and functional characterization of a novel kg51 bifunctional cellulase/hemicellulase from black goat rumen. *J. Agric. Food Chem.* **2018**, *66*, 9034–9041. [[CrossRef](#)]
26. Patel, A.B.; Patel, A.K.; Shah, M.P.; Parikh, I.K.; Joshi, C.G. Isolation and characterization of novel multifunctional recombinant family 26 glycoside hydrolase from Mehsani buffalo rumen metagenome. *Biotechnol. Appl. Biochem.* **2016**, *63*, 257–265. [[CrossRef](#)]
27. Pai, C.K.; Wu, Z.Y.; Chen, M.J.; Zeng, Y.F.; Chen, J.W.; Duan, C.H.; Li, M.L.; Liu, J.R. Molecular cloning and characterization of a bifunctional xylanolytic enzyme from *Neocallimastix patriciarum*. *Appl. Microbiol. Biotechnol.* **2010**, *85*, 1451–1462. [[CrossRef](#)]
28. Tan, H.; Miao, R.; Liu, T.; Yang, L.; Yang, Y.; Chen, C.; Lei, J.; Li, Y.; He, J.; Sun, Q.; et al. A bifunctional cellulase–xylanase of a new *Chryseobacterium* strain isolated from the dung of a straw-fed cattle. *Microb. Biotechnol.* **2018**, *11*, 381–398. [[CrossRef](#)] [[PubMed](#)]
29. Gavande, P.V.; Nath, P.; Kumar, K.; Ahmed, N.; Fontes, C.M.; Goyal, A. Highly efficient, processive and multifunctional recombinant endoglucanase RfGH5\_4 from *Ruminococcus flavefaciens* FD-1 v3 for recycling lignocellulosic plant biomasses. *Int. J. Biol. Macromol.* **2022**, *209*, 801–813. [[CrossRef](#)]
30. Meng, Z.; Ma, J.; Sun, Z.; Yang, C.; Leng, J.; Zhu, W.; Cheng, Y. Characterization of a novel bifunctional enzyme from buffalo rumen metagenome and its effect on in vitro ruminal fermentation and microbial community composition. *Anim. Nutr.* **2023**, *13*, 137–149. [[CrossRef](#)]
31. Pavarina, G.C.; Lemos, E.G.d.M.; Lima, N.S.M.; Pizauro, J.M., Jr. Characterization of a new bifunctional endo-1, 4- $\beta$ -xylanase/esterase found in the rumen metagenome. *Sci. Rep.* **2021**, *11*, 10440. [[CrossRef](#)] [[PubMed](#)]
32. Gomez de Segura, B.; Fevre, M. Purification and characterization of two 1, 4-beta-xylan endohydrolases from the rumen fungus *Neocallimastix frontalis*. *Appl. Environ. Microbiol.* **1993**, *59*, 3654–3660. [[CrossRef](#)] [[PubMed](#)]
33. Chen, S.; Kaufman, M.G.; Miazgowiec, K.L.; Bagdasarian, M.; Walker, E.D. Molecular characterization of a cold-active recombinant xylanase from *Flavobacterium johnsoniae* and its applicability in xylan hydrolysis. *Bioresour. Technol.* **2013**, *128*, 145–155. [[CrossRef](#)] [[PubMed](#)]
34. Della Torre, C.L.; Silva-Lucca, R.A.; Ferreira, R.d.S.; Andrade Luz, L.; Oliva, M.L.V.; Kadowaki, M.K. Correlation of the conformational structure and catalytic activity of the highly thermostable xylanase of *Thermomyces lanuginosus* PC7S1T. *Biocatal. Biotransform.* **2021**, *41*, 81–92. [[CrossRef](#)]
35. Liu, Y.D.; Yuan, G.; An, Y.T.; Zhu, Z.R.; Li, G. Molecular cloning and characterization of a novel bifunctional cellobiohydrolase/ $\beta$ -xylosidase from a metagenomic library of mangrove soil. *Enzym. Microb. Technol.* **2023**, *162*, 110141. [[CrossRef](#)]
36. Han, C.; Yang, R.; Sun, Y.; Liu, M.; Zhou, L.; Li, D. Identification and characterization of a novel hyperthermostable bifunctional cellobiohydrolase-xylanase enzyme for synergistic effect with commercial cellulase on pretreated wheat straw degradation. *Front. Bioeng. Biotechnol.* **2020**, *8*, 296. [[CrossRef](#)]

37. Ren, W.; Zhang, F.; Yang, X.; Tang, S.; Ming, H.; Zhou, E.; Yin, Y.; Zhang, Y.; Li, W.J.C. Purification and properties of a SDS-resistant xylanase from halophilic *Streptomonospora* sp. YIM 90494. *Cellulose* **2013**, *20*, 1947–1955. [[CrossRef](#)]
38. Zhu, L.; Liu, C.; Li, Y.; Pan, K.; Ouyang, K.; Song, X.; Xiong, X.; Qu, M.; Zhao, X. Characteristics of recombinant xylanase from camel rumen metagenome and its effects on wheat bran hydrolysis. *Int. J. Biol. Macromol.* **2022**, *220*, 1309–1317. [[CrossRef](#)]
39. Zheng, F.; Huang, J.; Yin, Y.; Ding, S. A novel neutral xylanase with high SDS resistance from *Volvariella volvacea*: Characterization and its synergistic hydrolysis of wheat bran with acetyl xylan esterase. *J. Ind. Microbiol. Biotechnol.* **2013**, *40*, 1083–1093. [[CrossRef](#)]
40. Terrasan, C.R.F.; Guisan, J.M.; Carmona, E.C. Xylanase and  $\beta$ -xylosidase from *Penicillium janczewskii*: Purification, characterization and hydrolysis of substrates. *Electron. J. Biotechnol.* **2016**, *23*, 54–62. [[CrossRef](#)]
41. Kim, H.B.; Lee, K.T.; Kim, M.J.; Lee, J.S.; Kim, K.S. Identification and characterization of a novel KG42 xylanase (GH10 family) isolated from the black goat rumen-derived metagenomic library. *Carbohydr. Res.* **2018**, *469*, 1–9. [[CrossRef](#)] [[PubMed](#)]
42. Weimer, P.; French, A.; Calamari, T., Jr. Differential fermentation of cellulose allomorphs by ruminal cellulolytic bacteria. *Appl. Environ. Microbiol.* **1991**, *57*, 3101–3106. [[CrossRef](#)] [[PubMed](#)]
43. Kerley, M.; Fahey, G., Jr.; Gould, J.; Iannotti, E. Effects of lignification, cellulose crystallinity and enzyme accessible space on the digestibility of plant cell wall carbohydrates by the ruminant. *Food Struct.* **1988**, *7*, 59–65.
44. Bao, L.; Huang, Q.; Chang, L.; Zhou, J.; Lu, H. Screening and characterization of a cellulase with endocellulase and exocellulase activity from yak rumen metagenome. *J. Mol. Catal. B Enzym.* **2011**, *73*, 104–110. [[CrossRef](#)]
45. Fang, H.; Xia, L. Heterologous expression and production of *Trichoderma reesei* cellobiohydrolase II in *Pichia pastoris* and the application in the enzymatic hydrolysis of corn stover and rice straw. *Biomass Bioenergy* **2015**, *78*, 99–109. [[CrossRef](#)]
46. Billard, H.; Faraj, A.; Lopes Ferreira, N.; Menir, S.; Heiss-Blanquet, S. Optimization of a synthetic mixture composed of major *Trichoderma reesei* enzymes for the hydrolysis of steam-exploded wheat straw. *Biotechnol. Biofuels* **2012**, *5*, 9. [[CrossRef](#)]
47. Zhang, J.; Siika-Aho, M.; Tenkanen, M.; Viikari, L. The role of acetyl xylan esterase in the solubilization of xylan and enzymatic hydrolysis of wheat straw and giant reed. *Biotechnol. Biofuels* **2011**, *4*, 60. [[CrossRef](#)]
48. Dijkstra, J. Production and absorption of volatile fatty acids in the rumen. *Livest. Prod. Sci.* **1994**, *39*, 61–69. [[CrossRef](#)]

**Disclaimer/Publisher’s Note:** The statements, opinions and data contained in all publications are solely those of the individual author(s) and contributor(s) and not of MDPI and/or the editor(s). MDPI and/or the editor(s) disclaim responsibility for any injury to people or property resulting from any ideas, methods, instructions or products referred to in the content.